Dusty WISE sources interpreted with wise DUSTY models

Željko Ivezić
University of Washington
Robert Nikutta, Maia Nenkova, Nicholas Hunt-Walker, Moshe Elitzur

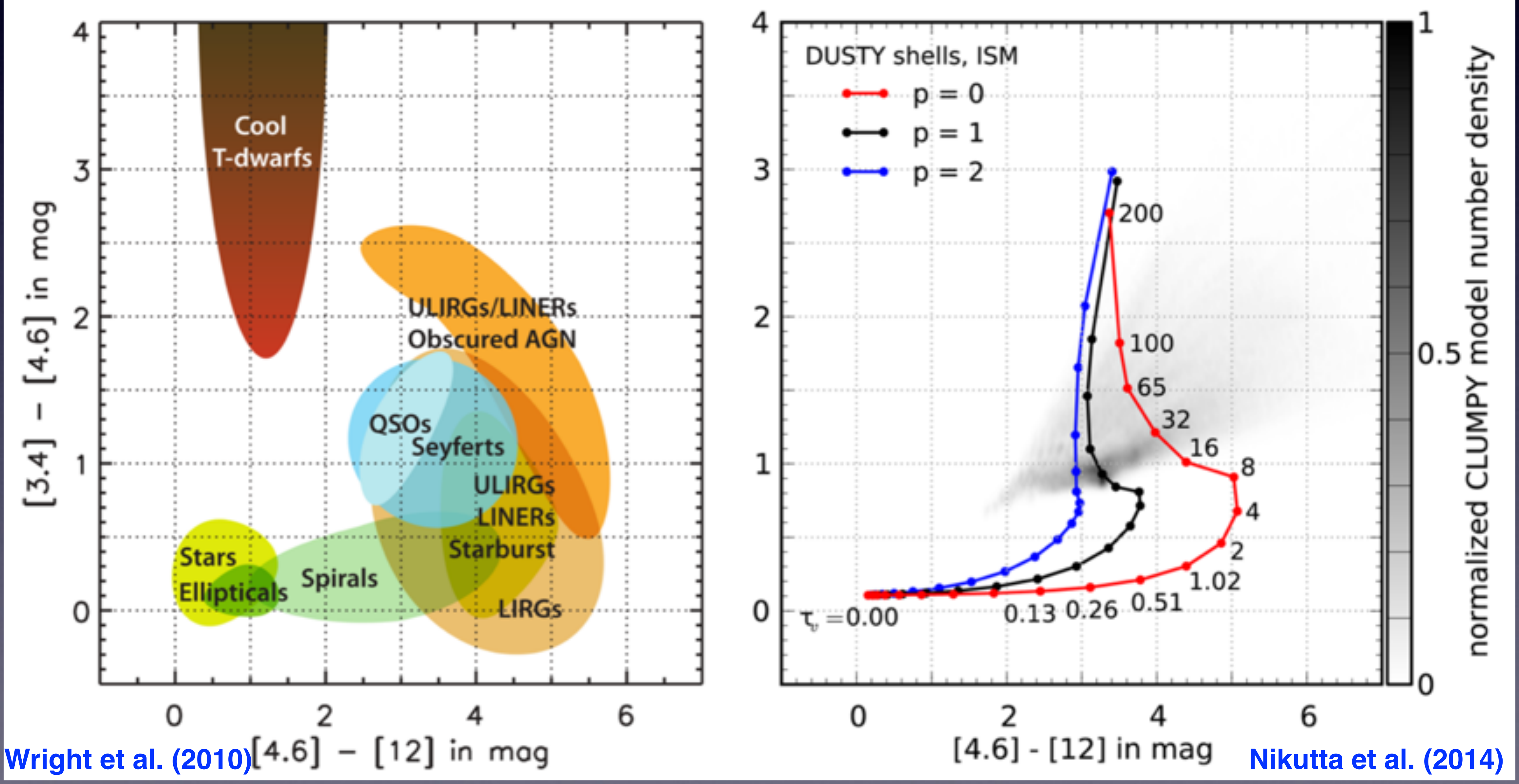

Wright et al. (2010)

Nikutta et al. (2014)

WISE at 5: Legacy and Prospects, Caltech, February 10-12, 2015

Outline

- Structure in WISE color-color diagrams as a consequence of the properties of the radiative transfer problem
- Association of the structure in WISE color-color diagrams with dusty shell properties
- Detailed analysis of WISE colors of Asymptotic Giant Branch (AGB) stars

And a brief advertisement…

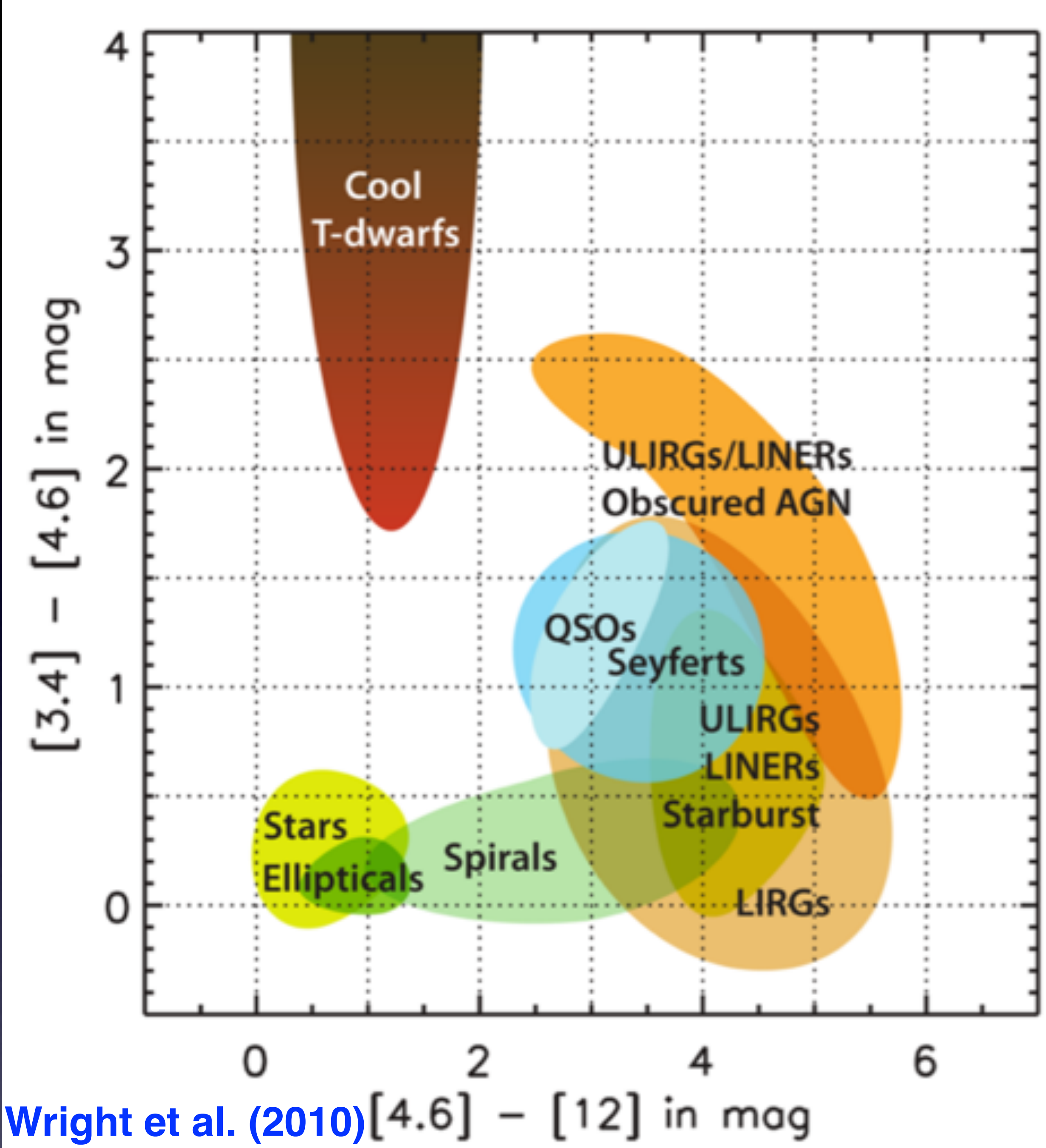

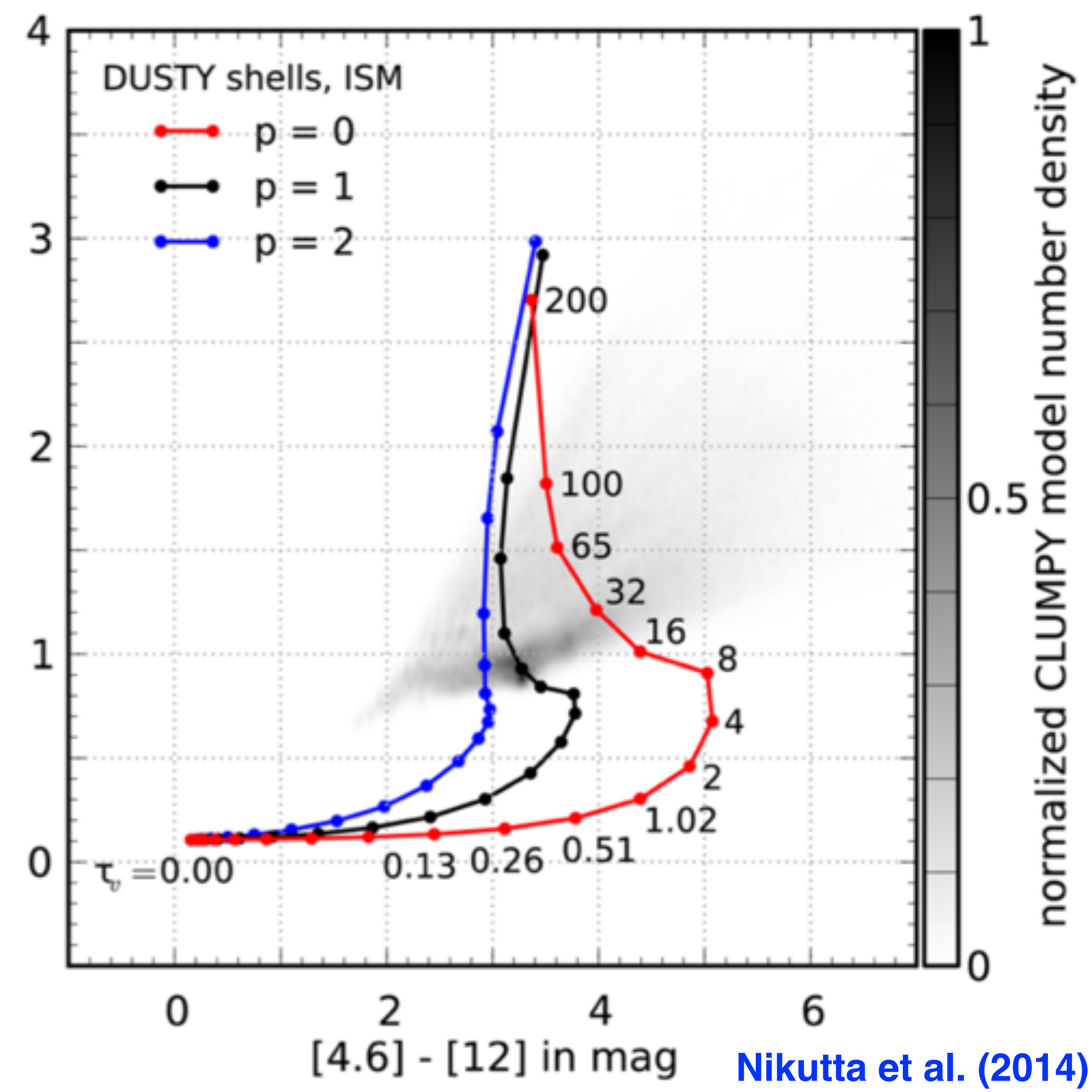

Various families of astronomical objects occupy different locations in the WISE color space; this is primarily a consequence of the scaling properties of the radiative transfer equation and varying dust density distributions (Ivezić & Elitzur 1997, 2000).

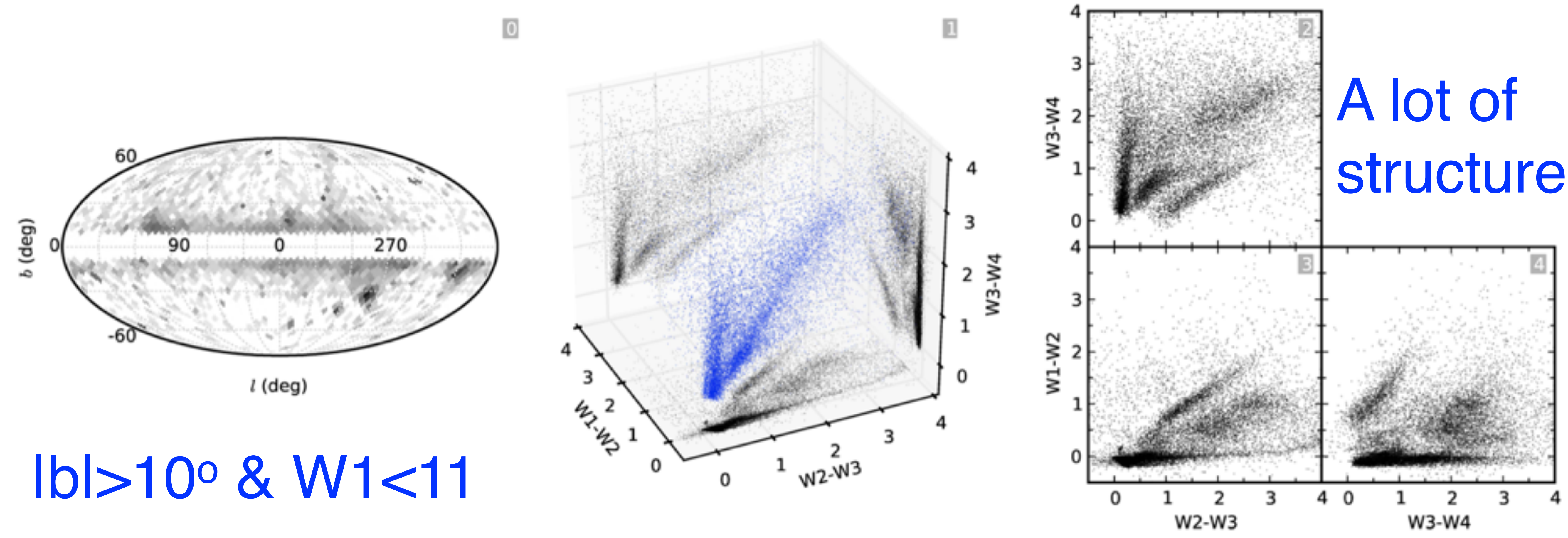

Figure 6. Distribution of 16 000 bright sources with Galactic latitude $|b| > 10°$ on the sky and in *WISE* colour space; see text for all selection criteria.

Structure in color-color diagrams is a result of **SCALING**

Density profile controls grouping, **FAMILIES DIFFER BECAUSE OF DUST DISTRIBUTION**

Within family, location is controlled by optical depth & dust properties

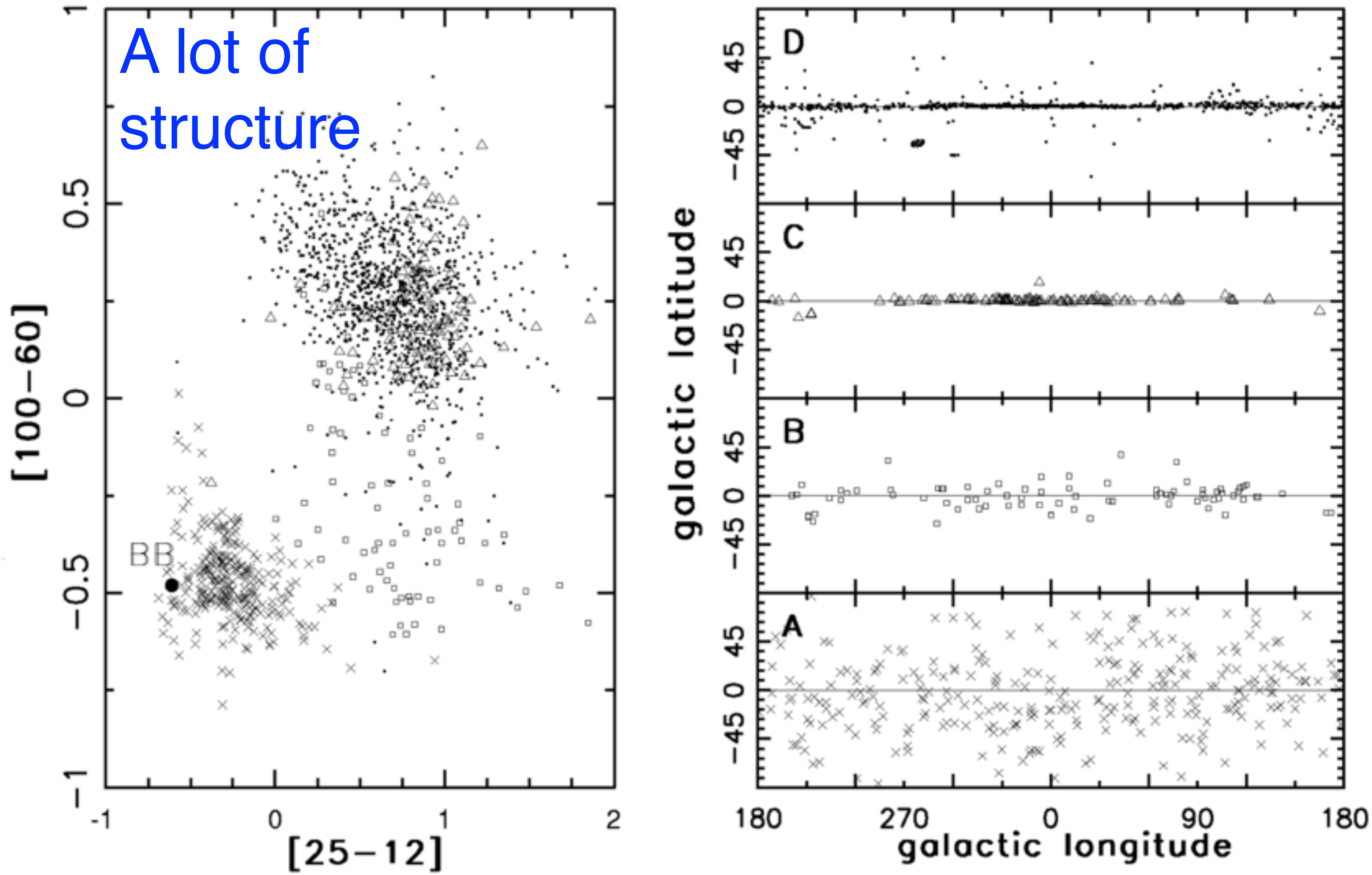

FIG. 2.—*Left:* [100–60]–[25–12] color-color diagram for all the Galactic *IRAS* sources free from cirrus contamination. The four classes identified by AutoClass are marked with different symbols: Class A (282 sources), crosses; B (80 sources), squares; C (119 sources), triangles; D (1013 sources), dots. The large dot marked BB denotes the colors of blackbody emission with temperature $T > 700$ K. *Right:* Galactic distributions of the four classes.

Ivezić & Elitzur (2000): strong correlation between IRAS colors and Galactic distribution (AGB stars and YSOs)

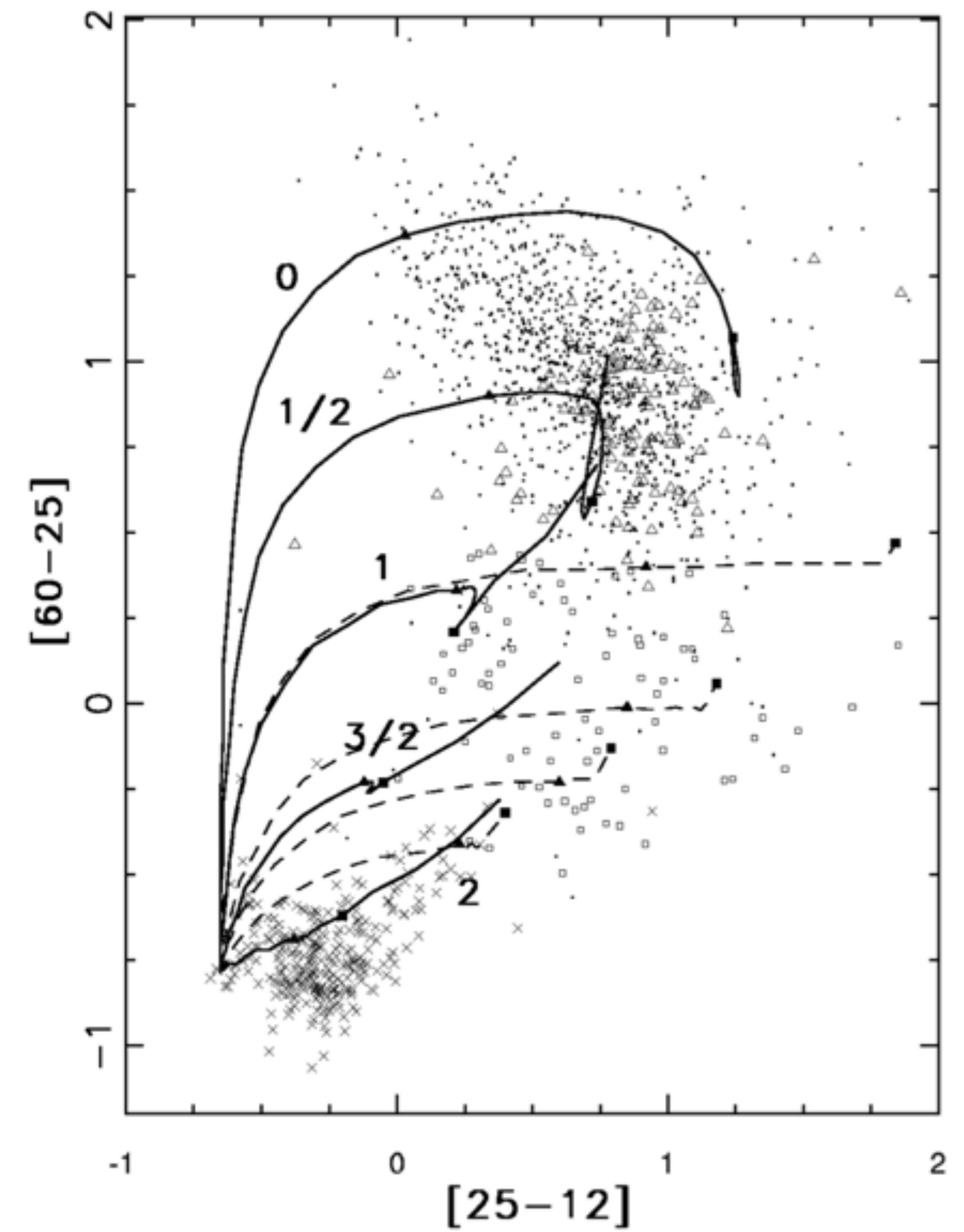

FIG. 3.—The [60–25]–[25–12] color-color diagram. Data are for the same sources presented in Fig. 2 using the same symbols. The full lines are model tracks for spherical dust shells with $T_1 = 1000$ K on their inner boundary and r^{-p} density profiles with $p = 0, \frac{1}{2}, 1, \frac{3}{2}$ and 2, as marked. The position along each track increases with dust optical depth τ_V away from the common origin $\tau_V = 0$ at the blackbody colors, with $\tau_V = 0.1$ marked by a filled triangle and $\tau_V = 10$ by a filled square. The end point for each track is $\tau_V = 100$. Dashed-line tracks show the effect on the $p = 2$ track of lowering T_1 to 300 (*lowermost track*), 200, 150, and 100 K (*uppermost track*). These tracks end at $\tau_V = 10$.

- Structure in IRAS color-color diagrams is a consequence of the properties of the radiative transfer problem
- The structure in IRAS color-color diagrams can be associated with the properties of dusty shells
- Can we do the same for WISE color-color diagrams?
- Yes, see Nikutta et al. (2014, MNRAS 442, 3361–3379)

The total flux is due to the attenuated (extincted) central source and the dusty shell (scattering and emission):

$f_\nu = f^*_\nu \exp(-\tau_\nu) + F^d_\nu/F$ where bolometric flux: $F = \int F_\nu \, d\nu$

f_ν depends on:

type of dust grains (cross sections)

overall optical depth

normalized density profile

f_ν DOES NOT depend on:

dimensions of the system

density scale

luminosity of central object

For detailed discussion, see Ivezić & Elitzur (1997, 2000) and code DUSTY

Primary Input:

- $q_\lambda = \kappa_\lambda/\kappa_{\lambda o}$ (chemistry, size)
- $\eta(y)$ (dynamics!)
- $\tau^T(\lambda_0)$ (…)

Secondary Input:

- $T_{sublimation}$
- r_2/r_1 (age/size)

$Q_{abs}(\lambda) + Q_{sca}(\lambda)$

for C and Si dust:

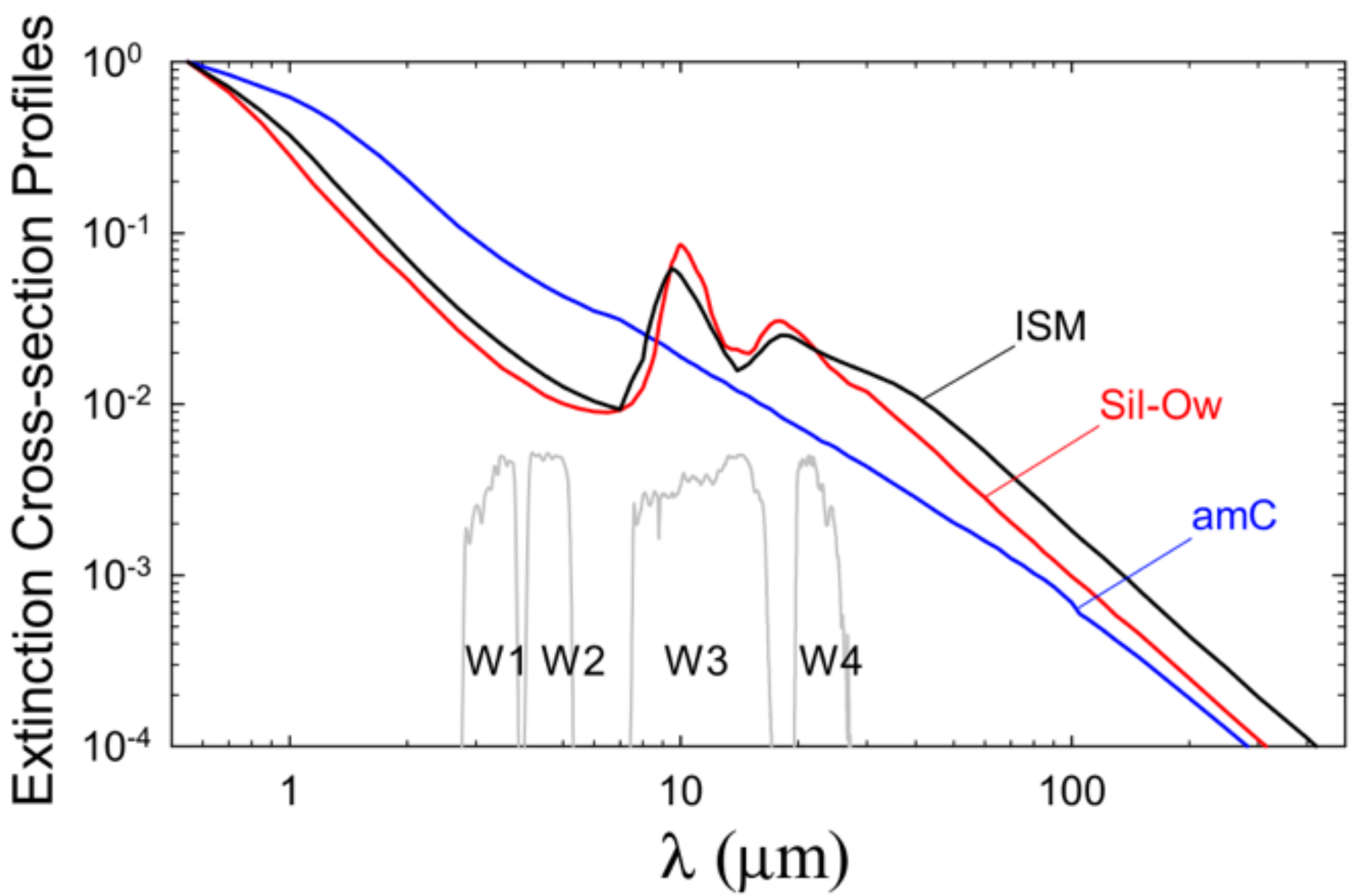

Figure 12. Extinction cross-sections, normalized to unity at 0.55 μm, of model dust for spherical grains with an MRN size distribution. Black: standard ISM dust mixture from Ossenkopf et al. (1992) and Draine (2003). Red: warm silicates from Ossenkopf et al. (1992) (Oss-w). Blue: amorphous carbon from Hanner (1988) (amC). The shapes of the *WISE* filter response functions are outlined in light grey.

Input for Modeling:

Star: T_{star}

Shell: $\rho(r)$, r_1, r_2

Dust: ρ_d/ρ, $p(a)$,

$Q_{abs}(\lambda)$, $Q_{sca}(\lambda)$, T_{sub}

Output:

SED: $f_\lambda = F_\lambda / F$

Surface Brightness (λ)

Top: uniform dust distribution

Bottom panel: $1/r^2$

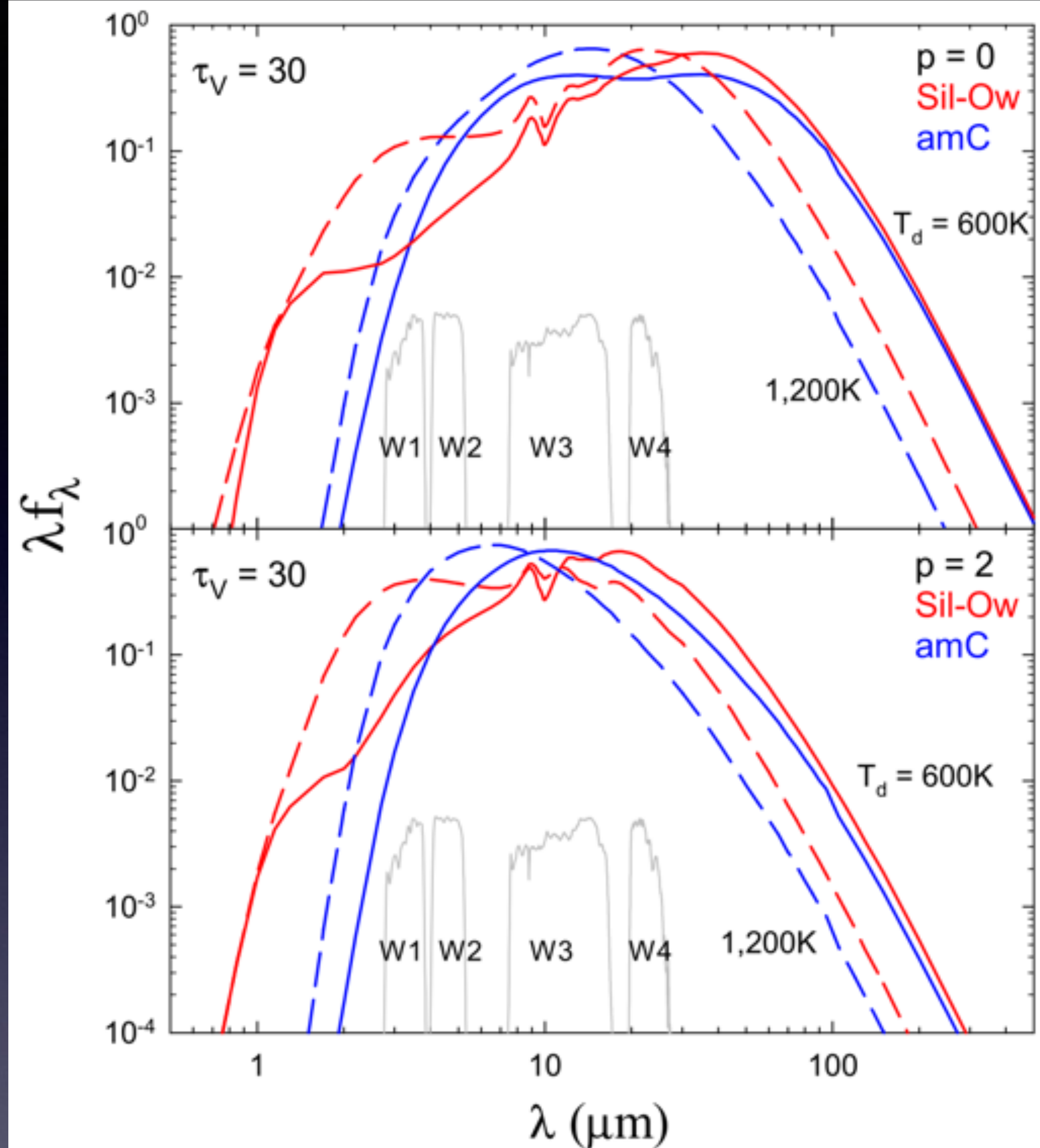

Figure 13. Model SEDs for spherical dust shells, centrally heated by a 10 000 K source. Silicate dust models are shown in red, amorphous carbon in blue. In both cases the grains follow the MRN size distribution and the extinction profiles are shown in Fig. 12. The shell optical depth is $\tau_V = 30$ at visual, its relative thickness is $Y = 100$ and its temperature on the inner boundary is either $T_d = 600$ K (solid lines) or $T_d = 1200$ K (dashed). The density profiles are power-law r^{-p} with $p = 0$ and 2, as marked. The shapes of the *WISE* filter response functions are outlined in light grey.

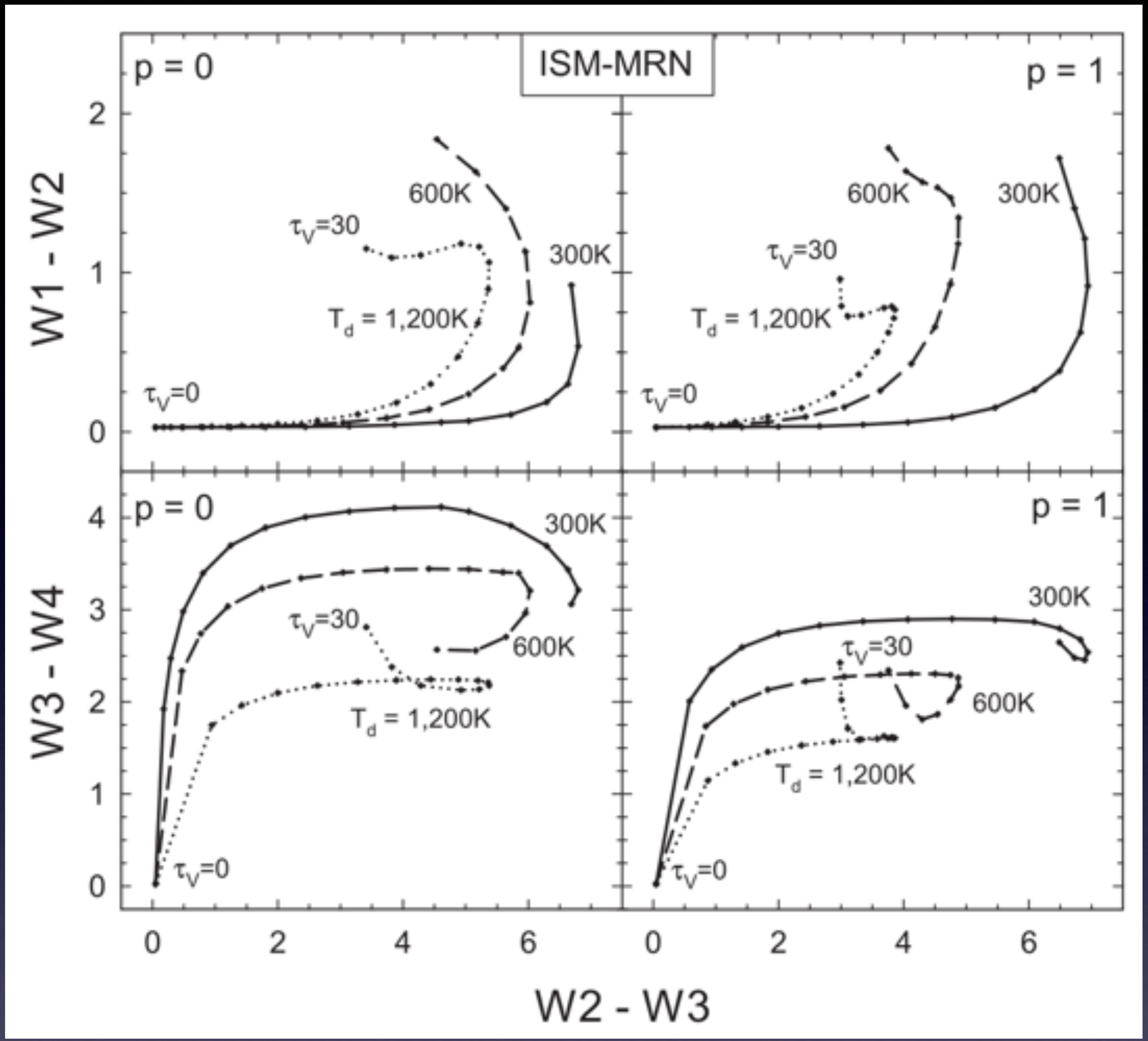

Colors (f_ν) primarily depend on:

- type of dust grains (a "track")
- overall optical depth
- normalized density profile
- (T_{dust} at the inner boundary)

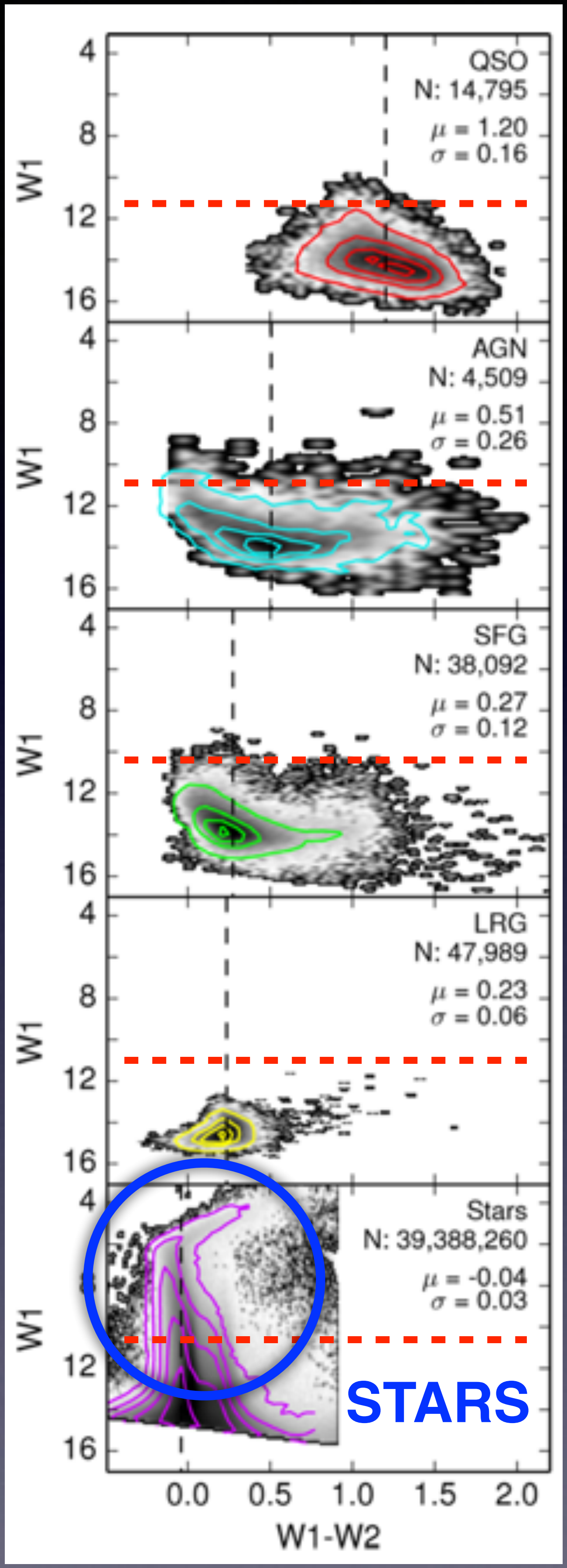

SDSS: W1<11 are Galactic sources!

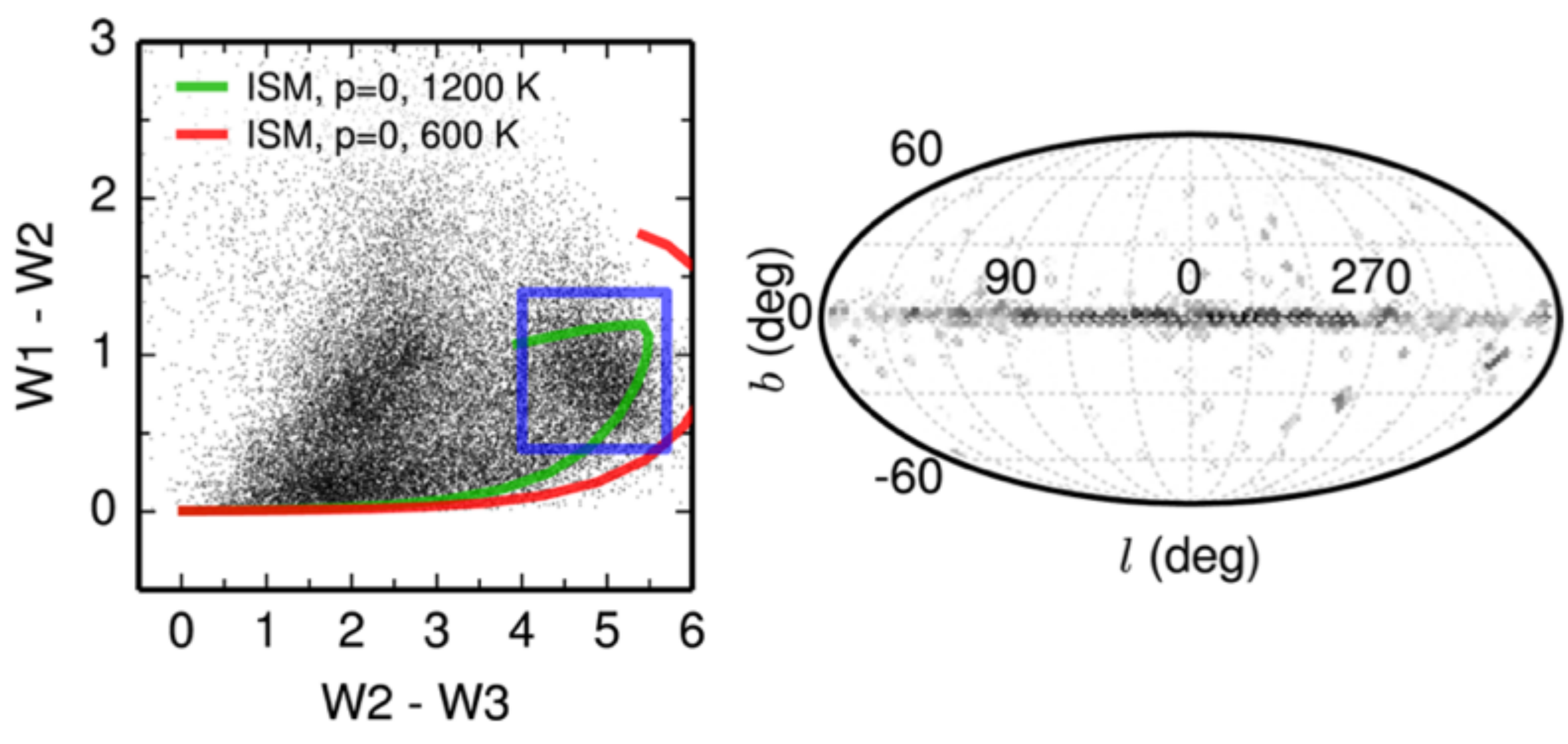

Figure 16. Identifying YSOs in the *WISE* data base. Left: distribution of

An example: Young Stellar Objects (OR flared disks!)

ISM dust grains

optical depth, $\tau_V < 10$

uniform dust density profile

T_{dust} ~ 1200 K

Evidence for at least some PNe (Koenig & Leisawitz 2014)

AGB stars: can separate O-rich from C-rich using only WISE colors!

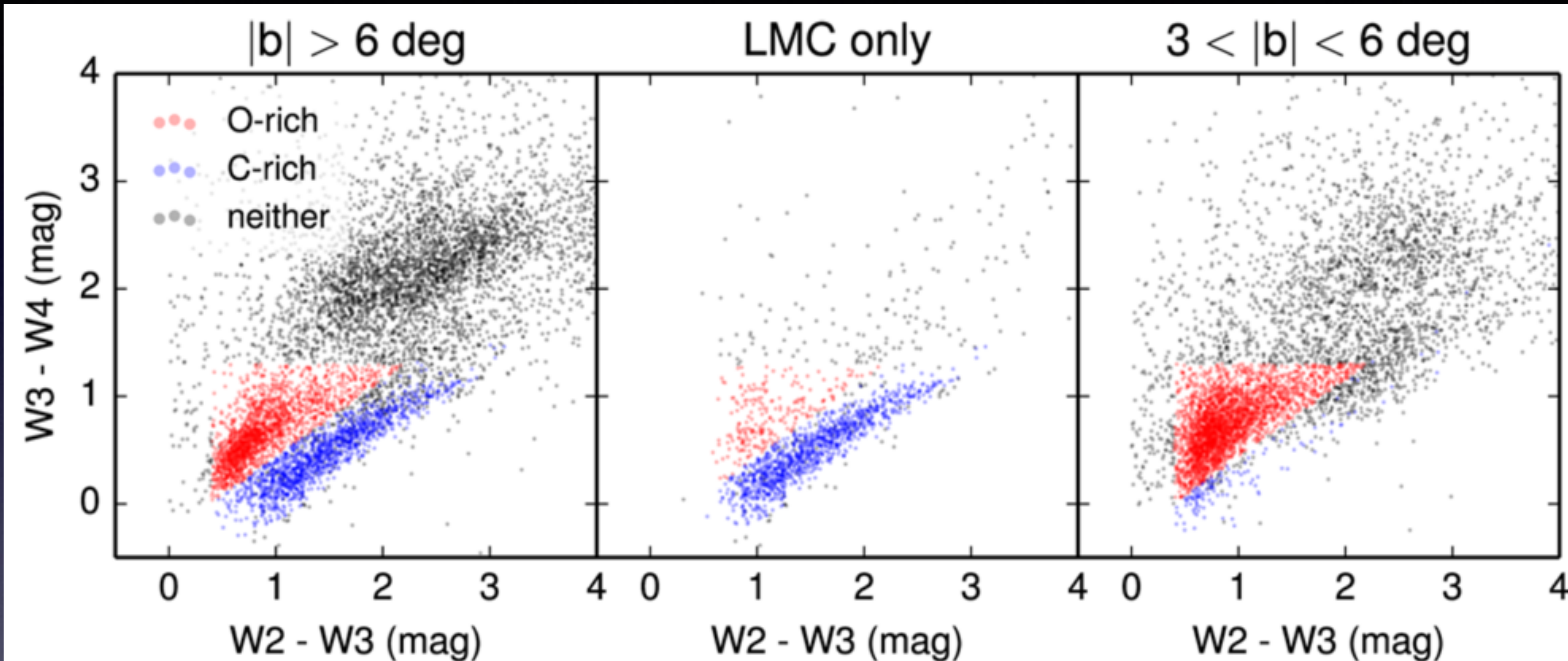

It is known from earlier work (e.g. Cioni 2009) that AGB stars from the LMC are dominated by C-rich population (blue points), while O-rich stars (red points) dominate Galactic AGB stars.

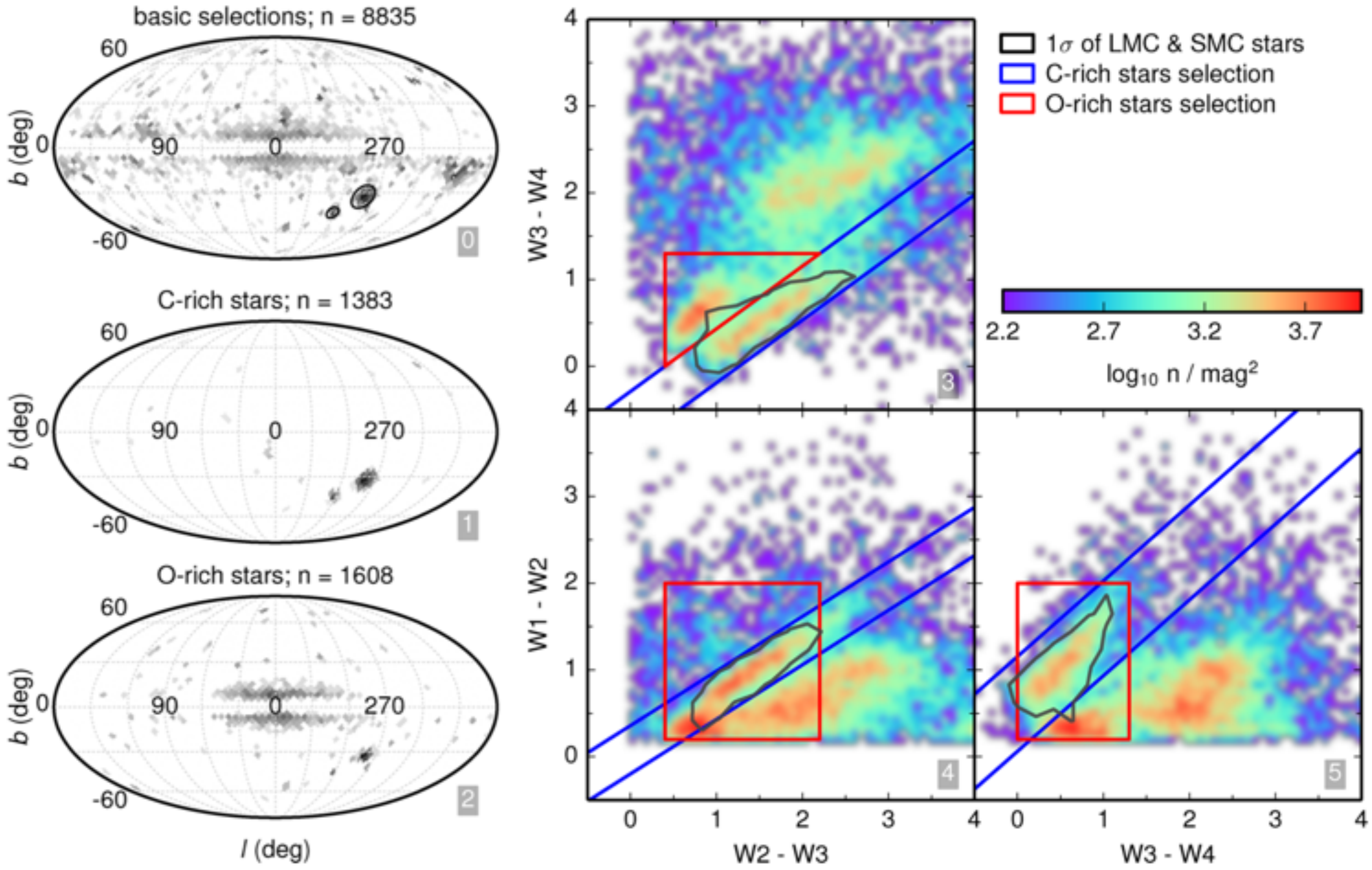

Figure 8. Selection of AGB stars. Each panel is numbered in its lower right corner. (0) All-sky map of bright sources with IR excess in Mollweide projection.

Used full WISE sample to optimize selection boundaries. WISE-based selection favors dusty AGB stars (samples selected using near-IR photometry, e.g. 2MASS and DENIS, are strongly biased against dusty AGB stars).

Tu & Wang (2012, arXiv:1207.0294) claim W1-W2~1.5 and W2-W3~0.5 corresponds to C stars, in conflict with our results

X. Tu & Z. Wang

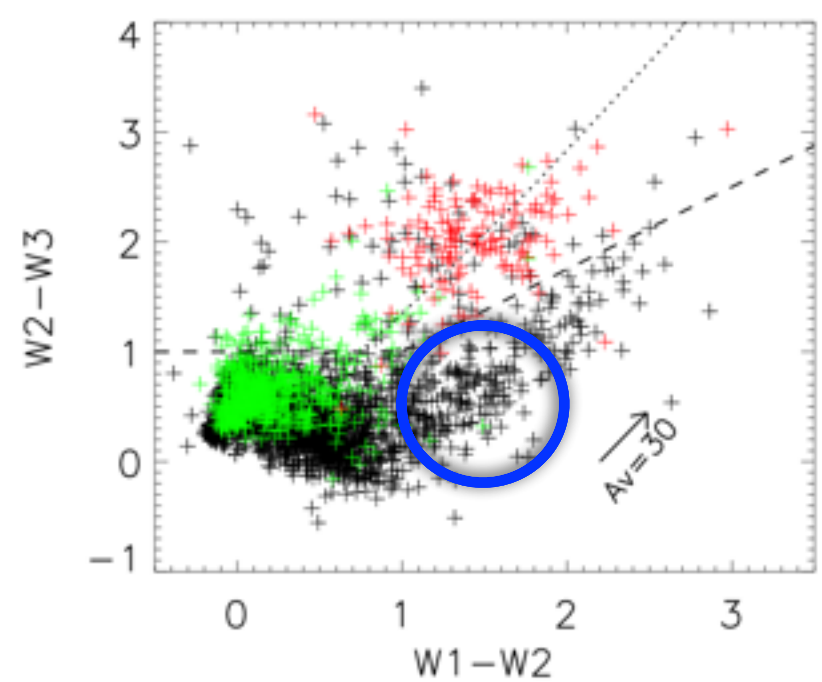

Fig.5 WISE color-color diagram of the known C-rich stars (black), AGB stars (green), and OH/IR stars (red). The dotted curve indicates the colors for objects at different low temperatures (Wright et al., 2010), indicating that the OH/IR stars have temperatures 500–800 K. The dashed lines can generally separate the OH/IR and a small fraction of the AGB stars from the C-rich stars in our sample.

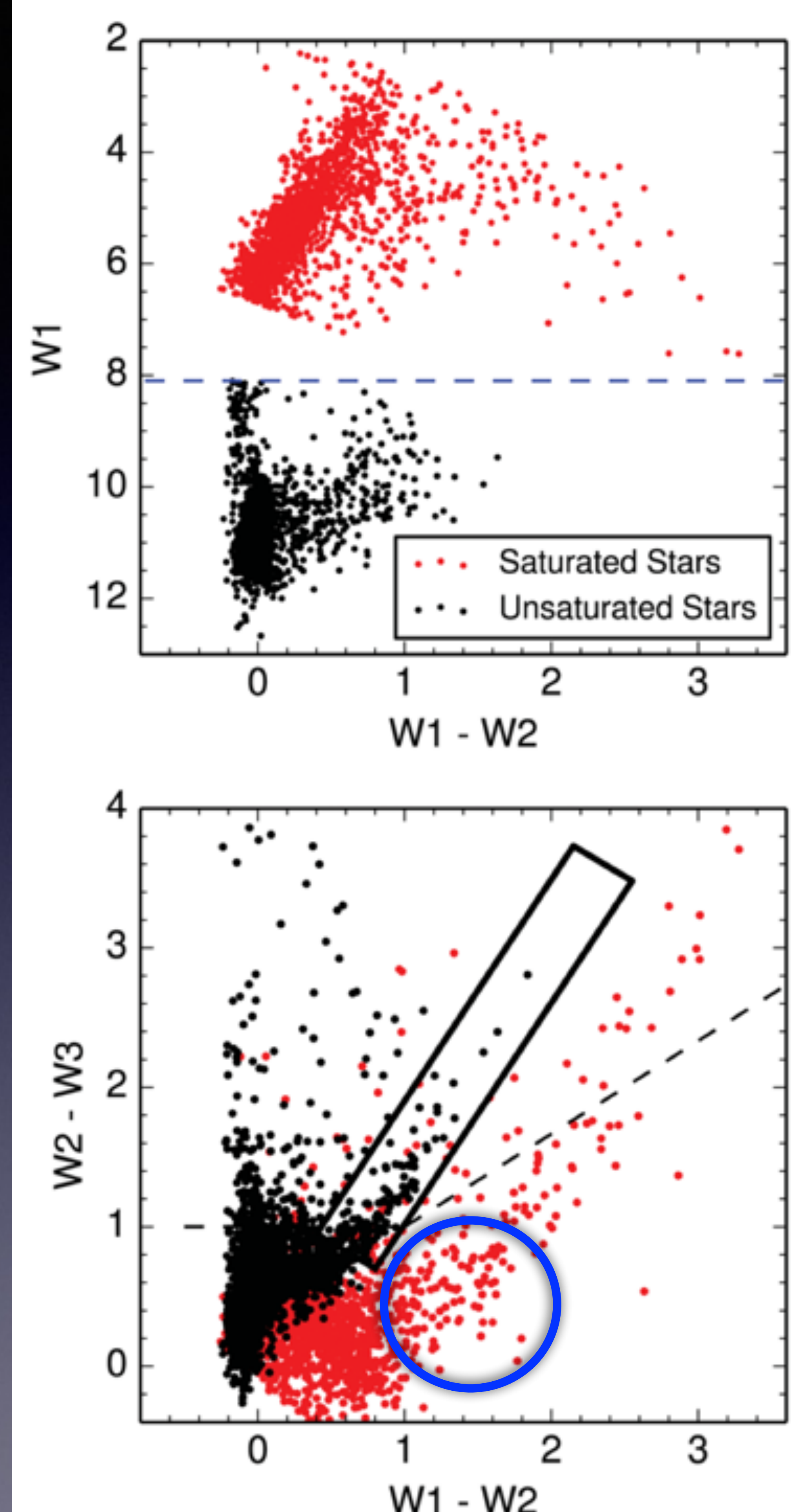

Resolution: need to reject saturated sources!

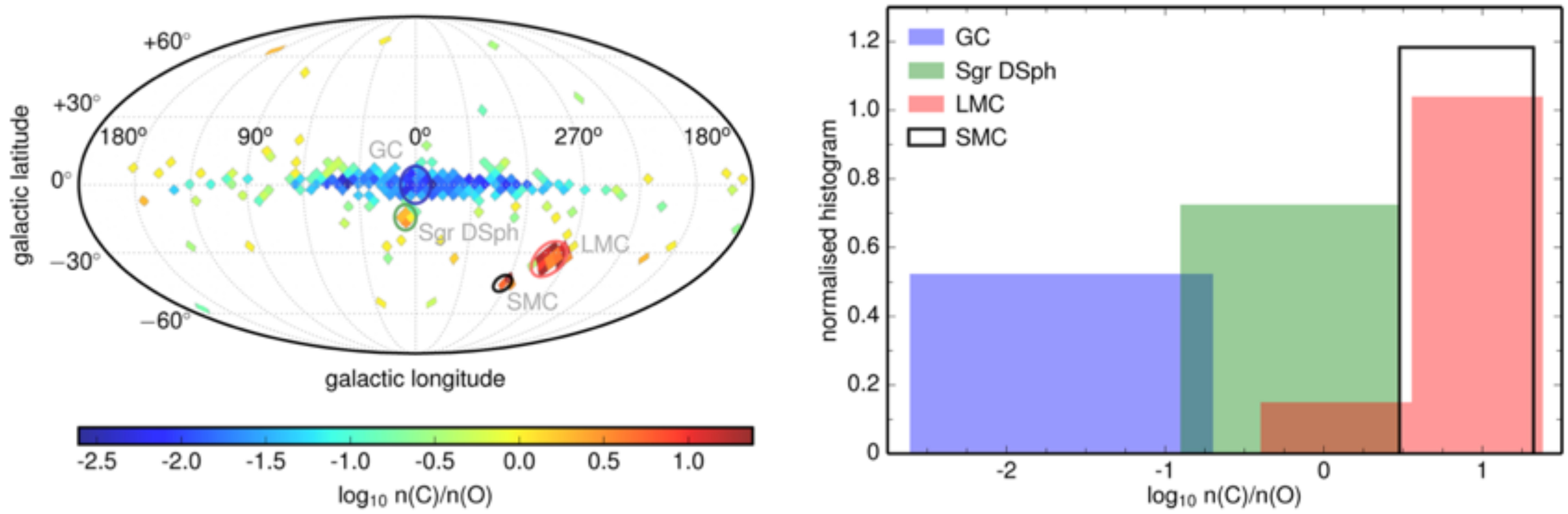

Figure 10. Left: all-sky map of the local C-to-O-rich star number ratio, in Mollweide projection. The Galactic Centre is at (0,0). This map is a ratio of Panels 1 and 2 in Fig. 8, but without the $|b| > 6°$ criterion. The colour scale shows the logarithm of the ratio per 13.43 deg^2 coordinate bin (defined by the HEALPIX tessellation). The locations of the Galactic Centre and three Milky Way satellites are indicated with (projected) circles. Right: distribution of $\log_{10}$ n(C)/n(O) in each circular area from the left panel. The histograms were obtained using Bayesian Blocks (see text). See Table 2 for statistics.

All-sky map for the C-to-O AGB star count ratio (above) reveals differences between the Galactic disc, the Magellanic Clouds and the Sgr Dwarf Spheroidal galaxy.

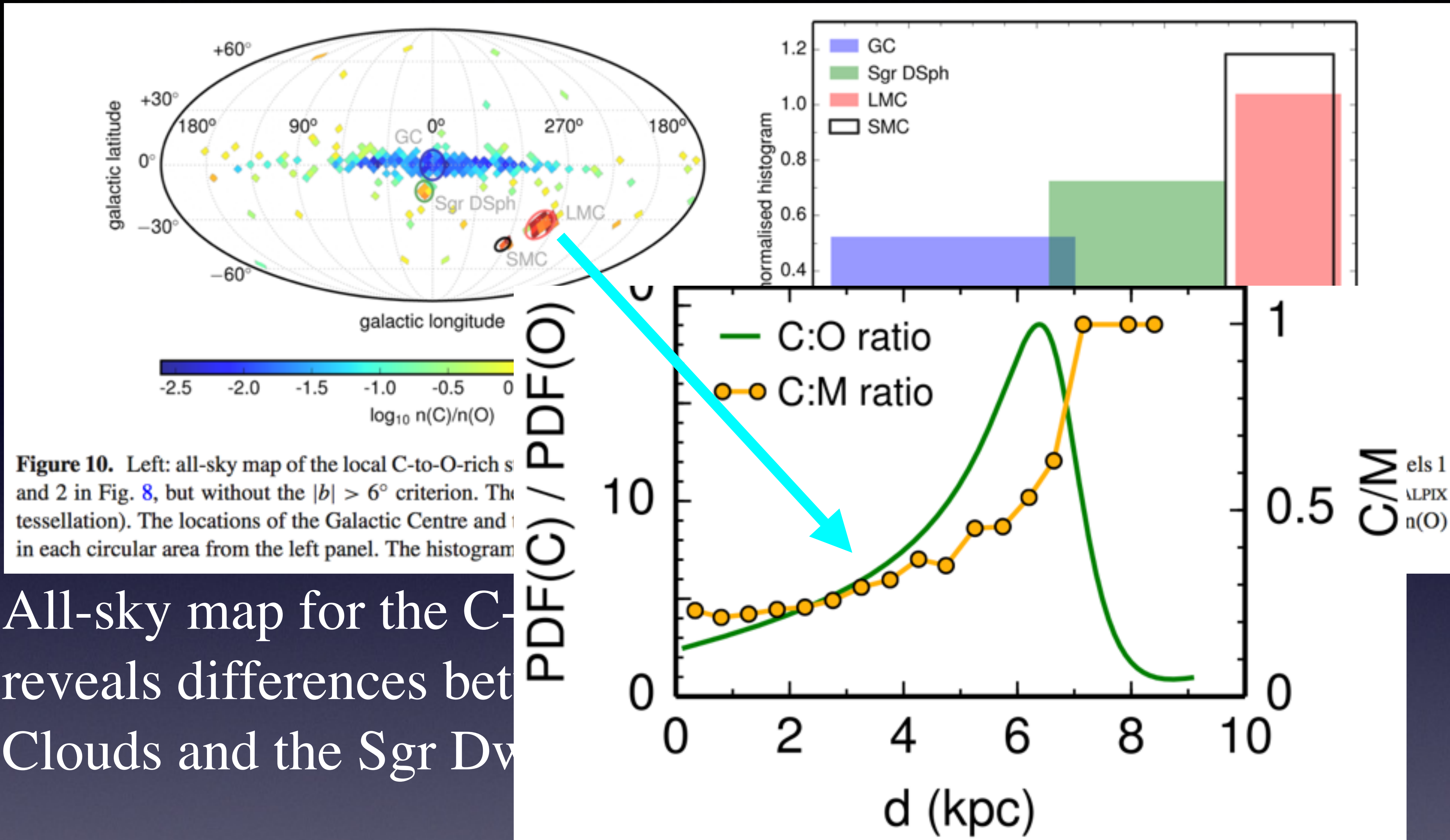

All-sky map for the C-
reveals differences bet
Clouds and the Sgr Dw

A radial gradient in the LMC disc is robustly detected: the C:O number ratio for dusty AGB stars increases with distance from the LMC center about twice as fast as measured for near-IR selected samples of early AGB stars. Interpretation “pending”…

Radially exponential disk. No sign of cutoff claimed for other tracers at 15-20 kpc

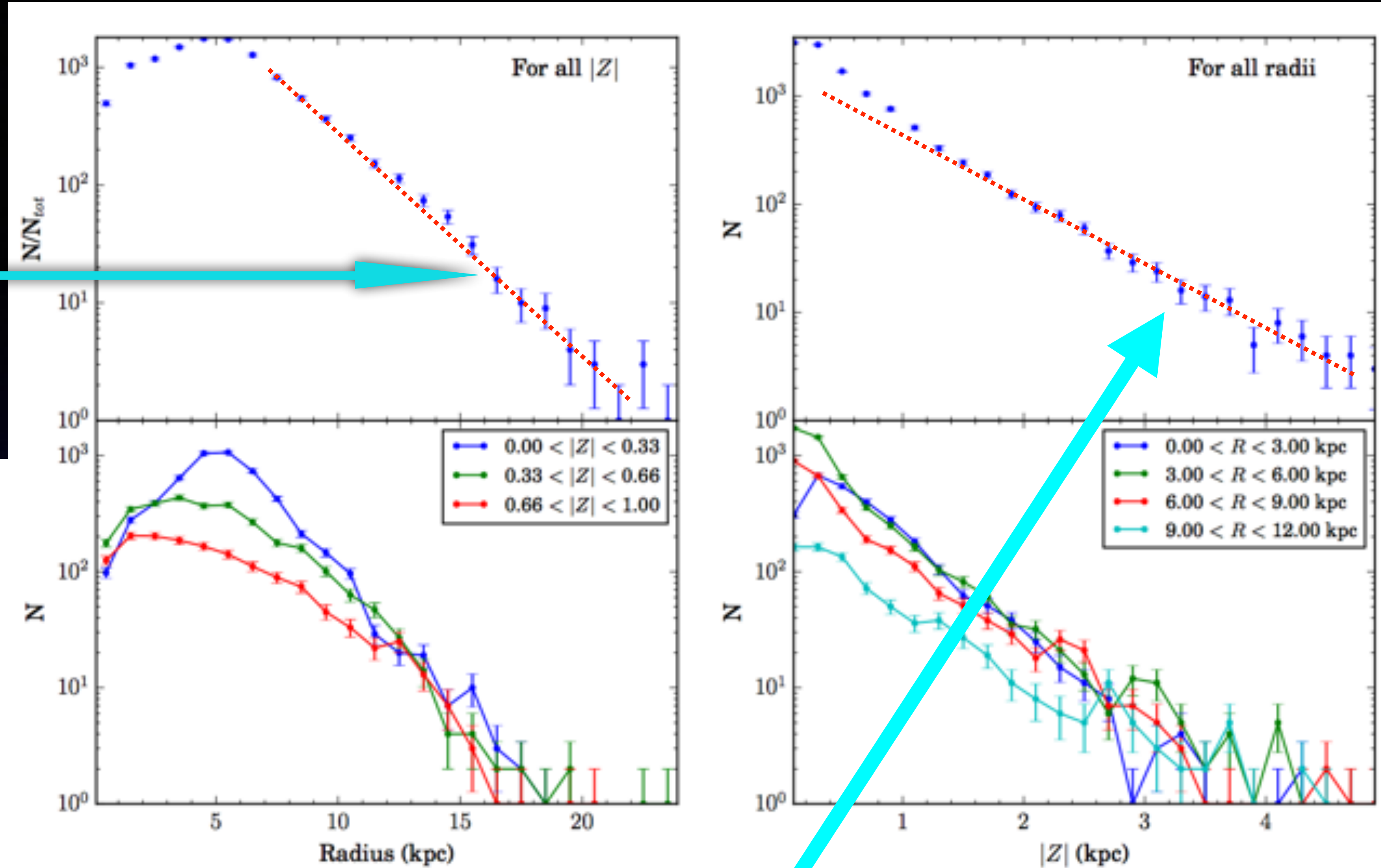

The furthest detection (Z~5 kpc) of the thick disk (H~750 pc) away from the Galactic plane!

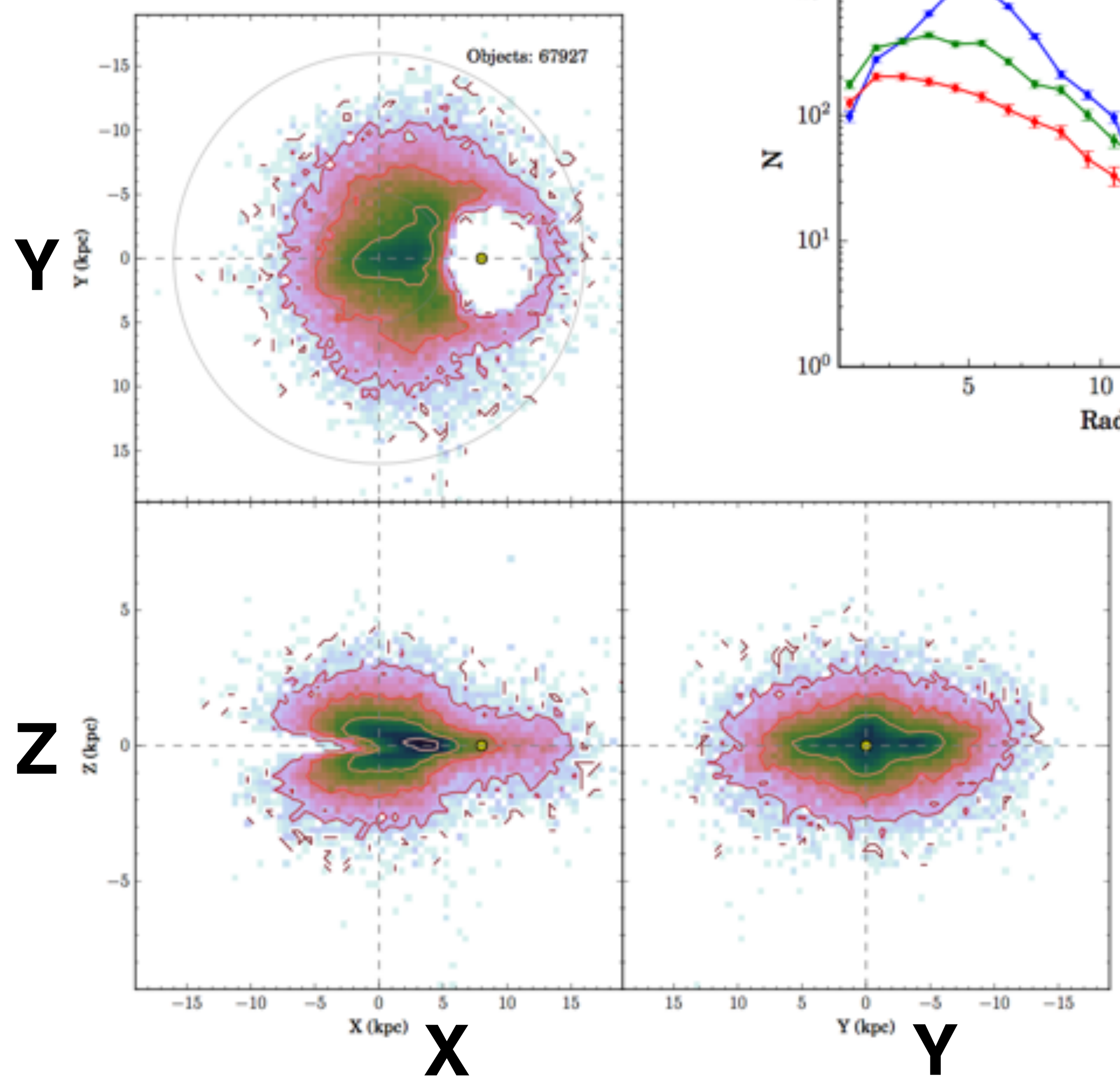

Figure 5: X-Y-Z distributions of the ALLWISE AGB candidate sample's O-rich stars. The Sun is set as the yellow dot with (X,Y,Z) = (8.0 kpc, 0 kpc, 0 kpc). The gray dashed lines mark (0,0) in each plot, and the contours are spaced by 0.75 logarithmically, starting at 0.

Hunt-Walker et al. (in prep)

Statistical analysis of massive datasets, e.g. WISE

- New skills required: traditional astronomy programs (still) do not place (enough) emphasis on statistical and computer science tools that are mandatory in survey astronomy

Data mining and knowledge discovery

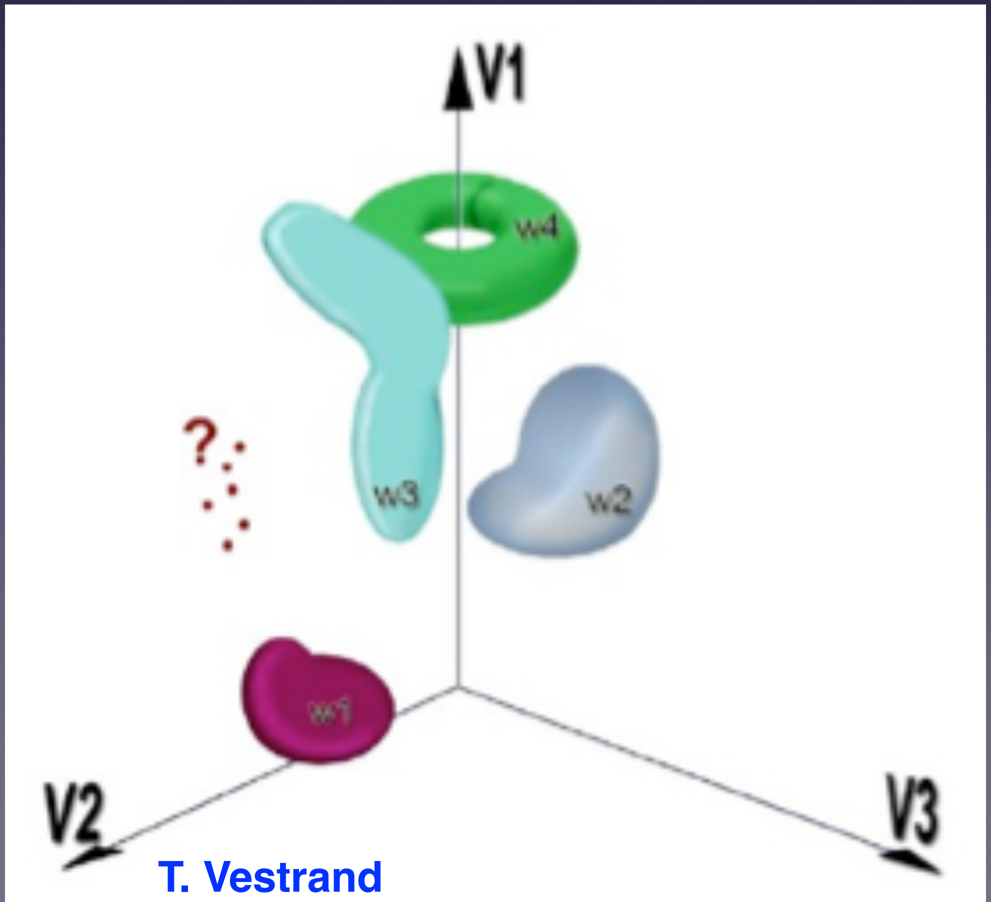

- High-D spaces with [m,b]illions of points
- Characterization of known objects
- Classification of new populations
- Discoveries of unusual objects

Clustering, classification, outliers

Statistics, Data Mining and Machine Learning in Astronomy

Željko Ivezić, Andrew Connolly, Jacob Vanderplas, Alex Gray

Princeton University Press, 2013

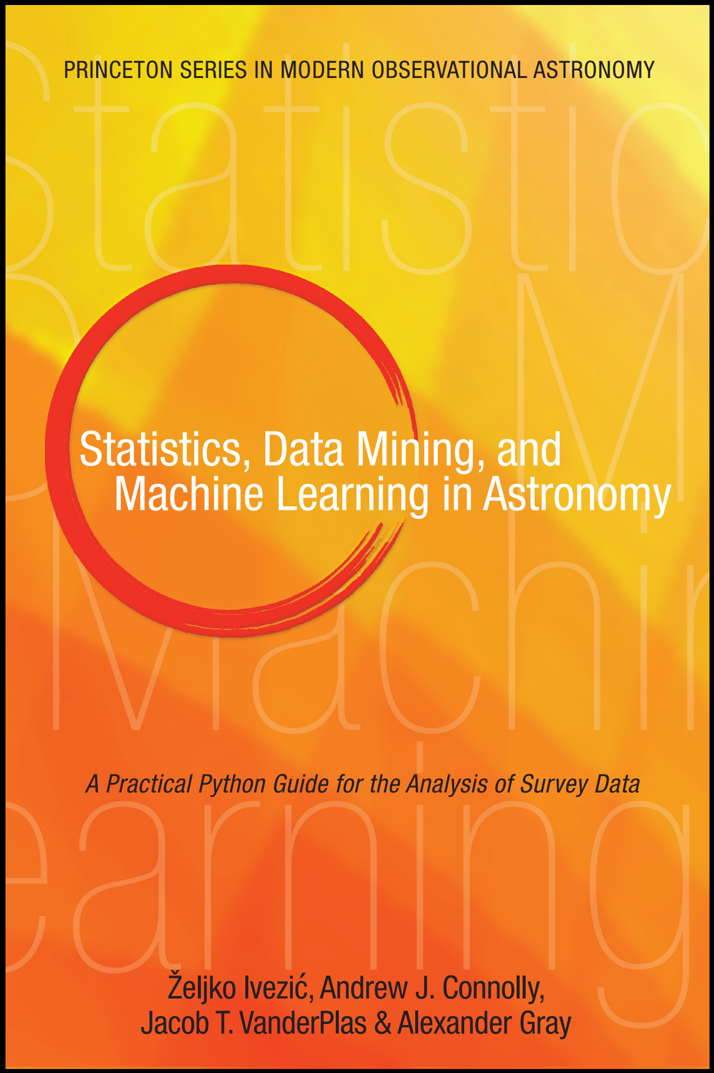

- Complete *Practical* guide to statistical analysis, data exploration, and machine learning
- Example-driven approach, using real data (SDSS, LIGO, LINEAR, WMAP, and others)
- All book figures and examples generated in python (matplotlib), with code available online – for free!
- Makes use of *numpy, scipy, matplotlib, scikit-learn, pymc, healpy,* and others
- Supporting python package: *astroML*

New book

News

October 2012: astroML 0.1 has been released! Get the source on Github

Our Introduction to astroML paper received the CIDU 2012 best paper award.

Links

astroML Mailing List

GitHub Issue Tracker

Videos

Scipy 2012 (15 minute talk)

Citing

If you use the software, please consider citing astroML.

AstroML: Machine Learning and Data Mining for Astronomy

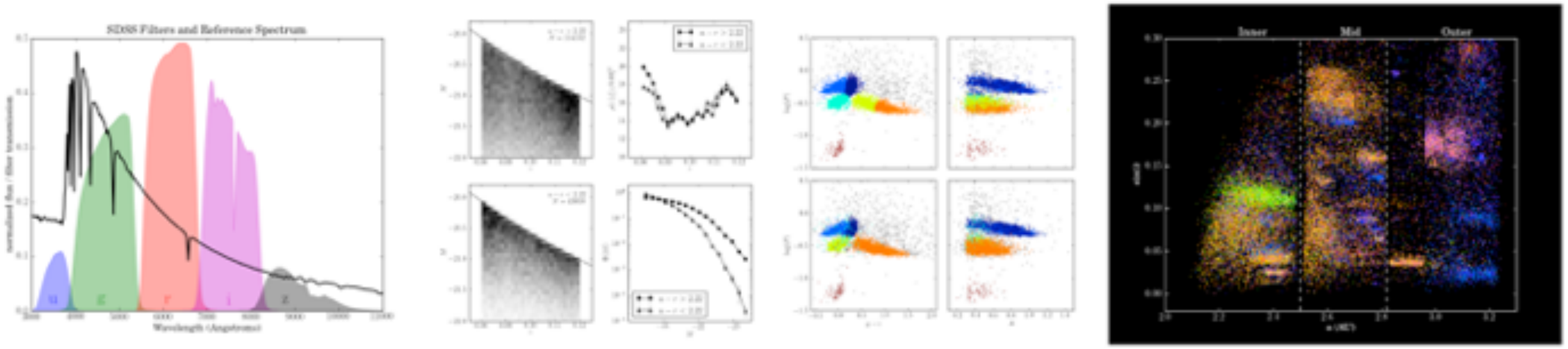

AstroML is a Python module for machine learning and data mining built on numpy, scipy, scikit-learn, and matplotlib, and distributed under the 3-clause BSD license. It contains a growing library of statistical and machine learning routines for analyzing astronomical data in python, loaders for several open astronomical datasets, and a large suite of examples of analyzing and visualizing astronomical datasets.

Downloads

- Released Versions: Python Package Index
- Bleeding-edge Source: github

The goal of astroML is to provide a community repository for fast Python implementations of common tools and routines used for statistical data analysis in astronomy and astrophysics, to provide a uniform and easy-to-use interface to freely available astronomical datasets. We hope this package will be useful to researchers and students of astronomy. The astroML project was started in 2012 to accompany the book **Statistics, Data Mining, and Machine Learning in Astronomy** by Zeljko Ivezic, Andrew Connolly, Jacob VanderPlas, and Alex Gray, to be published in late 2013. The table of contents is available here: `here(pdf)`.

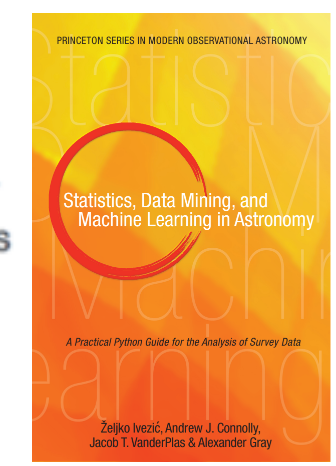

User Guide

1. Introduction

- 1.1. Philosophy

Open source!
www.astroML.org

Textbook Figures

This section makes available the source code used to generate every figure in the book *Statistics, Data Mining, and Machine Learning in Astronomy*. Many of the figures are fairly self-explanatory, though some will be less so without the book as a reference. The table of contents of the book can be seen **`here(pdf)`**.

Figure Contents

Each chapter links to a page with thumbnails of the figures from the chapter.

Chapter 10: Time Series Analysis

This chapter covers the analysis of both periodic and non-periodic time series, for both regularly and irregularly spaced data.

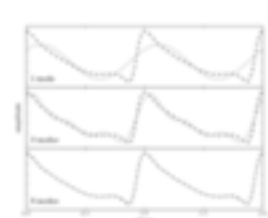

Fourier Reconstruction of RR-Lyrae Templates

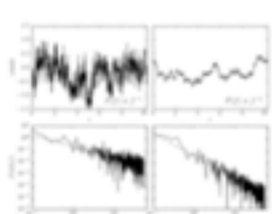

Generating Power-law Light Curves

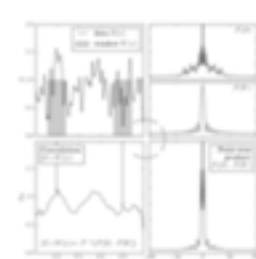

Plot a Diagram explaining a Convolution

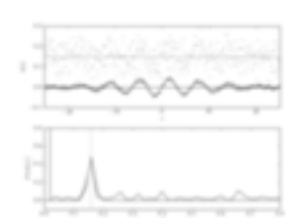

Fast Fourier Transform Example

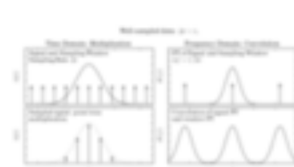

The effect of Sampling

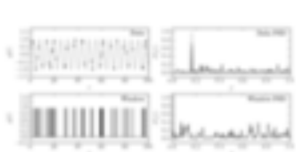

The effect of Sampling

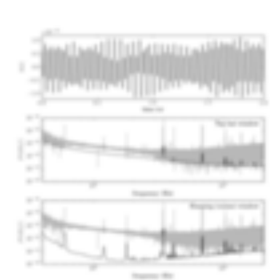

Plot the power spectrum of the LIGO big dog event

Examples of Wavelets

Conclusions:

1) various families of astronomical objects occupy different locations in WISE color space; this is a consequence of the scaling properties of the radiative transfer equation and varying dust density distributions

2) Galactics WISE sources can be reliably separated from extragalactic WISE sources using only WISE data

3) asymptotic giant branch (AGB) stars with circumstellar dust shells can be selected using only WISE data and separated into O-rich and C-rich classes

4) an all-sky map for the C-to-O AGB star count ratio reveals differences between the Galactic disc, the Magellanic Clouds and the Sgr Dwarf Spheroidal galaxy, and a radial C-O ratio gradient in the LMC disc is robustly detected

Big thanks to the WISE team for producing this wonderful dataset!